SEMARAK ILMU PUBLISHING

Journal of Advanced Research in Fluid Mechanics and Thermal Sciences

Journal homepage:
https://semarakilmu.com.my/journals/index.php/applied_sciences_eng_tech/index
ISSN: 2462-1943

Parameter Study of Porosity Effects on Surface Temperature for a Porous Block Under Wind, Water Source and Thermal Radiation

Mohammad Yaghoub Abdollahzadeh Jamalabadi[1,*]

[1] Chabahar Maritime University, Chabahar 99717-56499, Iran

ARTICLE INFO

Article history:
Received 1 November 2022
Received in revised form 22 December 2022
Accepted 24 December 2022
Available online 31 December 2022

Keywords:
Porous media, sweat evaporation, clothed human body, radiant heat, thermo-physiology

ABSTRACT

Textiles play an essential role in human civilization due to their thermal comfort. Textiles which regulate heat transfer between the skin and the local environment shape body microclimates without wasting excess energy. Cloth design is important for human comfort and thermal physiology. The mass and heat transfer from the skin covering play an important role in human thermoregulation and engineering design of textile and dressing. Heat and moisture transfer due to sweating in a clothing system under sun radiation is performed in this study. Governing equations of mass, momentum, and energy balance for the air and water phases through the porous media are solved by finite element method. Results of temperature, pressure, water vapor concentration, and relative humidity for various time steps are analyzed. As well influence of relative humidity on drying behavior is studied. Finally based on the comfort temperature for skin surface the optimal porosity of medium is obtained. The method of current study can be used as an algorithm for cloth design for various environmental and material properties for specified human comfort standard. Especially, the time domain analyses show that the optimal configurations perform better for low porosity ratios.

1. Introduction

The study of thermo-physiology and thermal protection of a clothed body requires mass transfer due to perspired moisture transport in a clothing system [1]. Textiles serve as a thermal barrier as well as a means of expressing personal identity and aesthetics. Water dissipation in permeable porous media is a significant cycle in many industries. Numerous actual impacts should be thought of liquid stream, heat move and transport of taking an interest liquids and gases [2]. These impacts are unequivocally coupled, and predefined interfaces can be utilized to display these impacts [3]. The development of science and technology has led to more diverse properties being explored for textiles in fields such as medical, firefighting, aerospace, and military applications. Examples include bacterial resistance, flame retardancy, lightness, breathability, and waterproofness. Despite all the different textile properties, the primary function of textiles, regardless of how human society evolves, has

* *Corresponding author.*
E-mail address: abdollahzadeh@dongguk.edu

https://doi.org/10.37934/araset.29.1.295315

always been to adapt thermal comfort to different ambientes. A human's thermal comfort range is 37 °C around, which is a constant temperature for endotherms. Previous research focused on moisture transmission without taking into account the effects of liquid perspiration or external heat radiation [4]. The body must sweat when it is subjected to high levels of physical exertion, such as during athletics, with the goal of cooling the body by perspiration evaporation. As a result, the garment must be able to transmit a lot of moisture. However, at particularly high levels of activity, the fabric may not be able to instantly transport all of the perspiration produced to the atmosphere.

To learn about the mechanisms of sweat evaporation, build-up, and dripping in those who are constantly sweating. The average density of active glands is about 125–200 glands/cm2. The number of functional pores per cm2 is 213 in forearm, 177 in upper arm, 377 in dorsum of hand, 151 in chest, 30 in back, 99 in leg, 284 in thenar eminence, 167 in forehead, 21 in zygomatic arch, and 16 in buccal [5]. Those gland in a clothed body system act as a source of water which the various distribution of the sweat gland in several areas make a difference in cloth design [6]. The cloth must hold extra sweat for eventual drainage, and the fibre should not feel wet to the wearer. As a result, sportswear must have excellent air, water, and heat transmission, as well as water storage capabilities. It's hard to design a textile that has both good liquid storage and transmission qualities. As well, based on various conditions sweat rate is different for an un-acclimatized case the value of one litre per hour is maximum while the value for a well-acclimatized person is twice or more (with less NaCl content) [7]. To comprehend sweat drainage of the clothed body, the idea of dressed wetness was studied in some references [8]. The results revealed that as perspiration rate grew, the evaporation rate of the clothed body increased, and this increase may be explained by parameters (e.g., material composition, hydrophilicity, and evaporative resistance), which influenced sweat accumulation ability [9].

For athletic apparel, single layered cotton sewed textures is liked as these have more prominent versatility and stretch capacity contrasted with woven textures. Be that as it may, the issue is during significant degree of sweat effort, the texture is wet as it assimilates the perspiration which isn't immediately sent to the climate. This causes an uneasiness to feel to the wearer [10]. Various substances can used as a cloth which have several thermal inertias, and sensation of heat or cold. Adjustments to the preset two-phase flow in cloth and environment medium are necessary when considering an unsaturated porous material. The changing water saturation inside the porous media is computed in this approach [11]. This model and instructions are based on the preceding version and focus on the additional processes needed to implement multiphase flow in porous media, along with evaporation from of the liquid to gaseous phase. The desired body temperature is 370C. If the designed cloth allows human body heat production to the environment it would be a good design. The 14-fold range of metabolisms and thermal sensors help skin in thermal management [12].

Trickling of fluid perspiration from the body or release of organic liquids cause moderately limited quantities of warmth trade, however openness to rain and different fluids in the climate can cause high paces of warmth misfortune and gain [13]. Dress is utilized external the skin to broaden the body's scope of thermoregulatory control and lessen the metabolic expense of thermoregulation [14]. It lessens reasonable warmth move, while as a rule allowing dissipated dampness (inert warmth) to get away. Bedclothes are a type of attire utilized for dozing [15]. Gauzes and other clinical covers may likewise be an uncommon instance of dress, controlling the warmth, dampness, and biotic exchange over a harmed skin [16]. This idea gives a concise depiction of the body's skin structure and thermoregulatory framework, trailed by a more itemized depiction of how warmth and dampness are moved at the skin's external limit, lastly, the solace ramifications of skin temperature and moistness [17]. Since skin qualities are not equitably disseminated across the outer layer of the whole body, it is valuable for clothing configuration to have this data introduced by individual body part, at

every possible opportunity. Since the temperature inclination between the skin surface and the climate reduces in warm climate, reasonable warmth move becomes lacking to eliminate the body's metabolic rate [18]. Vanishing of body dampness is an exceptionally proficient warmth evacuation measure, and accordingly complex physiological components have advanced to support vanishing under states of warmth stress, and to limit it when not, both to keep away from overcooling and to limit the measure of water lost by the body [19].

The porous polymers used in these coatings are typically hydrophobic and closed cell. Solar reflectance greater than 95% requires a thickness of 160 m. Sweat wicking and drying are hindered. A major personal thermoregulation pathway, moisture management, in hot, humid, and sunny conditions, is essential to wick sweat away from skin and evaporate it quickly so that heat can be dissipated, and the body can cool safely [20-30].

It is noted that the mass transfer diffusivity coefficient is orders of magnitude smaller than that of advection, leading to a longer transient time. This longer period highlights the importance of the transient shape factor for mass transfer, as compared to that of pressure transient cases. Therefore, understanding the transient behavior (early time) of the shape factor is necessary for accurate determination of the diffusive mass transfer, which occurs mostly in the transient period compared to the pseudo steady-state period [31-35].

This study is focused on the mathematical derivation of a dimensionless porosity for the mass diffusion process in the presence of advective flow in convection. In contrast to previous investigations, both advective and diffusive mass transfer processes are considered to derive the dimensionless porosity effect. The effect of matrix block size distribution is discussed and heterogeneity due to porosity intensity is incorporated into the present model. The transient (early time) and pseudo steady-state periods of the matrix–fluid interaction are characterized by prediction of the dimensionless porosity behavior with time. Results presented in this work can be applied to the proper implementation of the equivalent mass transfer porosity by the addition of variable porosity matrix distribution effects and in calibration of dual porosity models. Although textile design is important for human comfort and thermal physiology few studies are performed on porous media design of that textiles. In current study the effect of environmental parameter such as relative humidity and material properties such as porosity of textile media are discussed for the first time. The novelty of current research is to find an optimal porosity for a given medium. The results will help sensing applications, such as humidity sensor position or sweat rate sensing with cloth design.

2. Methodology

In this section, descriptions of the physical system along with the assumptions used to develop our model are introduced. The governing equations of the system are derived and the analytical solutions for matrix and fluid are presented. The governing equations for mass transfer in a porous system are derived and the solutions of these equations are utilized to investigate the effect of different porosity functions on the spread of water droplet. The dimensionless porosity for a repetitive element of the porous system is obtained using the analytical solutions of the coupled partial differential equations of the matrix and fluid. This model describes a laminar dry airflow through a porous medium containing water vapor and liquid water. The geometry and boundary condition of porous and environment domain are shown in Figure 1. The environmental climate temperature happens normally across exceptionally wide scope of temperatures and water fume pressures is 4.7 kPa but here the constant of 20oC is considered. As described in introduction the sun-oriented radiation is also considered here as much as 0.8 kW per square meter of skin surface and radiation into an ambient surrounding at 20°C. It is assumed that all liquid water captured in the

porous medium. Values of parameters are presented in Table 1. The porosity (a measure of tight fitted and loose fitted) is variable here. The dry air flow velocity (u0), for Skin model the sweating base plate is on 37°C. Sun light radiation value it could be measured by testing rig Hönle device sunlight. Simulation Sun light simulated by 700 W/m^2.

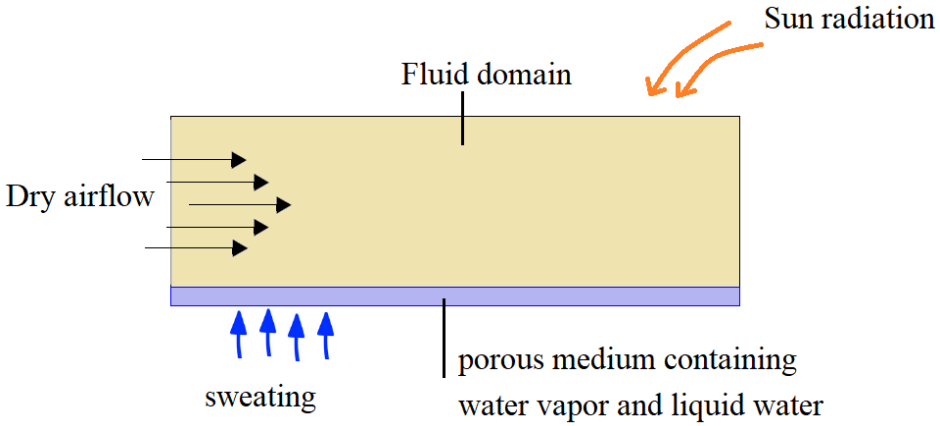

Fig. 1. Configuration of an evaporation cooling in porous media under continuous sweating, dry airflow, and radiative heat transfer

Table 1
Values of parameters

Parameter	Value	Unit	Description
p0	1	atm	Ambient pressure
T0	293.15	K	Ambient temperature
u0	0.1	m/s	Freestream velocity
csat	0.95914	mol/m³	Saturation vapor concentration at ambient temperature
D	2.6e-5	m²/s	Air-vapor Diffusivity at 298 K and 1 atm
H	2.454e6	J/kg	Latent heat of evaporation
K	1000	1/s	Evaporation rate
Sil	0.1	-	Irreducible liquid phase saturation
S0	0.5	-	Initial water saturation

2.1 Liquid-Gas Flow Through a Solid Matrix

The modelling of two-phase of liquid-gas flow inside a porous medium is different in many references but here the most common is used. In some models two coupled Single- phase flow in porous media is considered. In the most common references, the saturation parameters are used as the total index of phases is equal to one. If we consider α for the moist air (gaseous phase) then the value of water percentage (liquid phase) is equal to 1- α. It is good to notice that pore space is not fully saturated with water. The pressure inside the void volumes of the porous media called capillary pressure is the difference of pressure of gaseous phase and liquid phase (pc = pg − pl). The capillary between gaseous phase and liquid phase causes the flow motion (driving force). Here the capillary pressure is considered. As the effect exist through the different approaches the Brinkman Equations is used. Brinkman principle is used pressure distribution of moist air (pg) and applied as an additional pressure gradient (diffusion term) in the transport equation by the effective velocity of water as

$$\mathbf{u}_w = -\frac{\kappa_w}{\mu_w}\nabla p_g \qquad (1)$$

which includes the capillary effects. The subscription 'w' symbolized the water and subscription 'g' symbolized the moist air. the permeability (κ_w) and viscosity (μ_w) of the water. The above equation is used to calculate the flow field in the porous medium. The role of the porosity (ε) is considered indirectly in the permeability parameter as a fraction of the void space is filled by the air phase. The fluid stage speed is little contrasted with the wet air speed and to such an extent that Darcy's law is characterized as far as the gas stage constrain inclination to compute the water speed ul as per. It isn't important to characterize a second Darcy's law condition, however an extra vehicle condition for the fluid stage is required. Table 2 -4 contains air properties, liquid water properties, and water vapor properties respectively.

Table 2
Air properties

Parameter	Value	Unit	Description
Ma	0.028	kg/mol	Molecular weight of air
μa	1.81e-5	kg/(m·s)	Air viscosity at 20oC and 1atm
ka	0.025	W/(m·K)	Air thermal conductivity at 20oC and 1atm
Cp,a	1.006e3	J/(kg·K)	Air heat capacity at 20oC and 1atm
ρa	1.205	kg/m³	Air density at 20oC and 1atm

Table 3
Liquid Water properties

Parameter	Value	Unit	Description
Ml	0.018	kg/mol	Molecular weight
μl	1.002e-3	kg/(m·s)	Viscosity
kl	0.59	W/(m·K)	Thermal conductivity
Cp,l	4.182e3	J/(kg·K)	Heat capacity
ρl	998.2	kg/m³	Density

Table 4
Water Vapor properties

Parameter	Value	Unit	Description
Cp,v	2.062e3	J/(kg·K)	Vapor heat capacity
μv	1.8e-5	kg/(m·s)	Vapor viscosity
kv	0.026	W/(m·K)	Vapor thermal conductivity

2.2 Liquid Phase and Moisture Evolution

The cooperation of fluids with stringy fibrous materials might include one or a few actual wonders. Based on the overall sum of fluid included and the method of the fluid texture contact, the wicking cycles can be isolated into two gatherings: wicking from a limitless fluid supply (drenching, trans-planar wicking, and longitudinal wicking), and wicking from a limited (restricted) fluid repository (a solitary drop wicking into a texture). As indicated by fibre–fluid connections, the wicking cycles can likewise be partitioned into four classes: narrow entrance just; synchronous slender entrance and imbibition by the filaments (dispersion of the fluid into the inside of the filaments); slim infiltration and adsorption of a surfactant on filaments; and synchronous slim infiltration, imbibition by the strands, what's more, adsorption of a surfactant on filaments. When planning tests to re-enact fluid material connections of a functional cycle, it is fundamental to comprehend the essential cycles included and their energy.

One of the major boundaries which directs the fluid strong communications is the calculation of the strong, including the shape and relative places of the underlying parts in the framework, as unequivocally reflected in the Laplace pressure law showing that the pressing factor drop is relative to the trademark curves. Thusly, for similar material, its wetting conduct will be unique, sometimes definitely, when made into a film, a fibre, a fibre group or a stringy material, as exhibited in this part.

Mass of evaporation is obtained from linear relation of

$$m_{evap} = K_{evap}(A_w\ C_{v,sat} - C_v) \tag{2}$$

which saturation vapor concentration obtained from temperature; water activity is a function of moisture content on dry basis. By and large, it is a capacity relying upon the water content on dry premise of the encompassing air and the temperature, yet here an estimated worth of Aw = 0.9 is utilized due to the moderate variety of water content. One can incorporate the mechanistic formulations of the transport of Diluted Species interface, which settles for a focus in the extremely broad fluid flux variables. These equations (convection and diffusion of water vapor, dry air and water liquid) are utilized to depict the movement of the fluid stage (water) inside the permeable porous domain. The equation of evolution of moisture content is

$$\begin{aligned} \varepsilon\ \frac{\partial}{\partial t}\left(\alpha\rho_l + (1-\alpha)\rho_g\omega_v\right) + \rho_g\mathbf{u}_g\cdot\nabla\left(\frac{M_v\phi_w c_{sat}(T)}{\rho_g}\right) \\ + \nabla\cdot\left(-\rho_g D_{eff}\nabla\left(\frac{M_v\phi_w c_{sat}(T)}{\rho_g}\right)\right) \\ + \mathbf{u}_l\cdot\nabla\rho_l + \nabla\cdot\left(-D_w\frac{\partial}{\partial\phi_w}(\alpha\rho_l + (1 \\ -\alpha)\rho_g\omega_v)\nabla\phi_w\right) = 0 \end{aligned} \tag{3}$$

where

D_{eff} is $D_{va}\varepsilon_p^{4/3}s_g^{10/3}$ and evaporation source is $\frac{\partial[\varepsilon_p\rho_g\omega_v s_g]}{\partial t} + \rho_g\mathbf{u}_g\cdot\nabla\omega_v + \nabla\cdot\mathbf{g}_w$ The dissipation rate from the bare skin of the human body can be communicated as the dissipation rate from the naked skin, area is the skin region accessible for dissipation, the part of the body surface covered by water (skin wettedness), the mass exchange coefficient from the skin to the climate, soaked fume tension on the skin and the fume pressure in the climate. Sum of Molar fraction of air X_a and vapor X_v is 1 while Molar fraction of vapor obtained from ideal gas equation. Here diffusion coefficient of water is $1e^{-8}\times\exp\left(-2.8+2w(\phi_w)/\left(\varepsilon_p\rho_s\right)\right)$. The system to infer the exchange condition for water fume is like the past segment. Beginning from the protection condition and following the portrayal, one needs to execute the transition because of convection though the speed field is now known from the Brinkman condition and should be applied to the fume stage. The second vehicle instrument is motion because of paired dispersion of water fume and dry air in the vaporous stage. A typical connection for a viable diffusivity for two parts are in the accompanying table. Some investigation on manufactured and normal yarn materials in single pullover weaved textures, shows that some of water can absorb in textile causing the swelling. Such assumption is neglected here. As per the outcomes, it was reasoned that some samples showed quick wetting, less assimilation, extremely quick spread capacity of fluid dampness take-up, and higher upsides of aggregate single direction transportation.

2.3 Vapour Phase and Evaporation

Evaporative cooling noticed for various textiles. The dry cloth produced a more prominent temperature drop while the soaked cloth created a more noteworthy temperature drop subsequently. Generally wet attire can make cooling that is significantly more prominent than cooling created by water dissipating straightforwardly from the skin. As well, Initial cooling by wet textures is most noteworthy when a texture contains an insignificant measure of water while cooling is ideal throughout a more drawn-out timeframe when the texture contains undeniable degrees of water (soaked). The degree of cooling made by wet attire over the long haul is directed by the complete water content in the texture. This additionally clarifies why people as often as possible report further developed solace in hot conditions when wearing single-layered dress that doesn't assimilate a lot of sweat. The materials that ingest little water, for example, nylon and silk give quick cooling while cotton gives better cooling later.

Counting the dissipation interaction is finished by adding the mass of water fume that is vanished as source term in the vehicle condition. Dissipation happens, if the centralization of water fume is underneath the balance focus, which is dictated by the immersion fixation cast and water movement aw, with the water action depicts the measure of water that vanishes into air. The vanishing rate relies upon the material properties and the cycle that causes the dissipation. It should be picked with the goal that the arrangement isn't influenced if further expanded. This compares to expecting that fume is in balance with the fluid or, at the end of the day, the time scale for vanishing is a lot more modest than the littlest time size of the vehicle conditions. This is valid for pore estimates that are not very huge. The warmth of dissipation is then embedded as source term in the warmth move condition as per mass sources.

$$Q_{\text{evap}} = L_{\text{v}} G_{\text{evap}} \tag{4}$$

The conduction, convection, and radiation (long-wave and short-wave) are thermal exchange mechanisms at skin surface. The thermal management are assisted by moisture diffusing and sweat evaporating at skin surface.

$$Q = -\left[\left(C_{p,\text{v}} - C_{p,\text{a}}\right)\mathbf{g}_{\text{w}} + C_{p,1}\mathbf{g}_{\text{lc}}\right] \tag{5}$$

With the assumption that moisture molecules will diffuse along the surface of any intervening fibres, thus predicted the moisture diffusivity in non-hygroscopic nonwoven fabrics as

$$D_{eff} = D_a P + D_a\left(1 - V_f - P\right)(1 - P)/\left(1 + sV_f - P\right) \tag{6}$$

Genuinely great consistency of forecast results and test information suggests that utilizing both porosity and convolution is an adequate methodology in describing dampness dispersion through non-hygroscopic sinewy materials. Be that as it may, many ordinarily utilized filaments, for example cotton and fleece, are hygroscopic and the reactions of hygroscopic texture under dampness inclinations is considerably more mind boggling because of connections among dampness and strands.

2.4 Heat Balance

The Heat Balance equation is

$$\frac{DT}{Dt} = \alpha\left(\frac{\partial^2 T}{\partial x^2} + \frac{\partial^2 T}{\partial y^2}\right) \quad (7)$$

The still-air convective heat transfer coefficients for standing condition is (velocity < 0.1 m/s)

$$h = 1.21(T_{skin} - T_a)^{0.43} \quad (8)$$

and for seated condition is

$$h = 0.78(T_{skin} - T_a)^{0.56} \quad (9)$$

Based on the similarity between the fluid transport coefficients (Nusselt (h=Nu k_{fluid}/d) and Sherwood (hm = Sh D_{fluid}/d) numbers) one can calculate the mass transfer coefficients (h_m = h D_{fluid}/k_{fluid}). As well for the various segment of body (Foot, Lower leg, Thigh, Pelvis region, Head, Hand, Forearm, Upper arm, Chest, Back, Whole body) some constant reported as a heat transfer coefficient. Mixture laws, based on the amount of vapour and dry air, is used to characterize the thermodynamic properties of air with water vapor. Once Moist air is selected as the fluid type, this is done automatically, and the system of equations may be found in any Heat Transfer textbook. The concentration c (mol/m^3) from the transport equation is provided as an input term for water vapor. There is an option to define a single fluid type within the porous domain. But it will simplify the model too much. Implementing a two-phase flow requires defining the fluid type in a way that is appropriate for both gas and liquid phases. As a reason, the moist air qualities must be manually adjusted. For the sake of simplicity, all other properties of the material are also defined manually. Capillary rise in a fibrous material is another issue can happen. Soaking a fibre assembly differs from wetting a single fibre because the surface areas of the two are vastly different. Instead of dealing with a single dimension of fibre with specified radius, the study must deal with a medium made up of fibres and irregular pores with a complex surface structural geometry. But here in the sake of simplicity the porous media approach is adopted.

2.5 Porous Permability, Conduction and Diffusion

The absolute permeability is defined by the permeability of the porous matrix (i.e. κ). When two phases are present, the saturation affects the permeability of each phase. The accurate value of permeability can detect after examination of 3D porosity of utilitarian clothing through miniature tomography framework. The relative permeabilities κ_{rl} and κ_{rg} for the liquid and gaseous phases, respectively, define this, with $\kappa_l = \kappa\kappa_{rl}$ and $\kappa_g = \kappa\kappa_{rg}$. Relative permeability curves are frequently determined empirically or experimentally. The form of relative permeability contours is hugely affected by the porous material features and the liquids directly, and is often determined practically or practically. The parameters in this model are defined by the fact that they will be constantly positive values:

$$\kappa_{\mathrm{rg}} = \begin{cases} 1 - 1.1 s_l, & s_l < 1/1.1 \\ 0\,, & s_l \geq 1/1.1 \end{cases} \tag{10}$$

$$\kappa_{\mathrm{rl}} = \begin{cases} \left(\dfrac{s_{\mathrm{l}} - s_{\mathrm{li}}}{1 - s_{\mathrm{li}}}\right)^3, s_l > s_{\mathrm{li}} \\ 0\,,\ s_l \leq s_{\mathrm{li}} \end{cases}$$

The variable S_{li} is the complex liquid phase saturation, unfolding the fact that inside the porous medium the liquid phase will remain in saturation. Figure 2 presents relative permeability of gas and liquid.

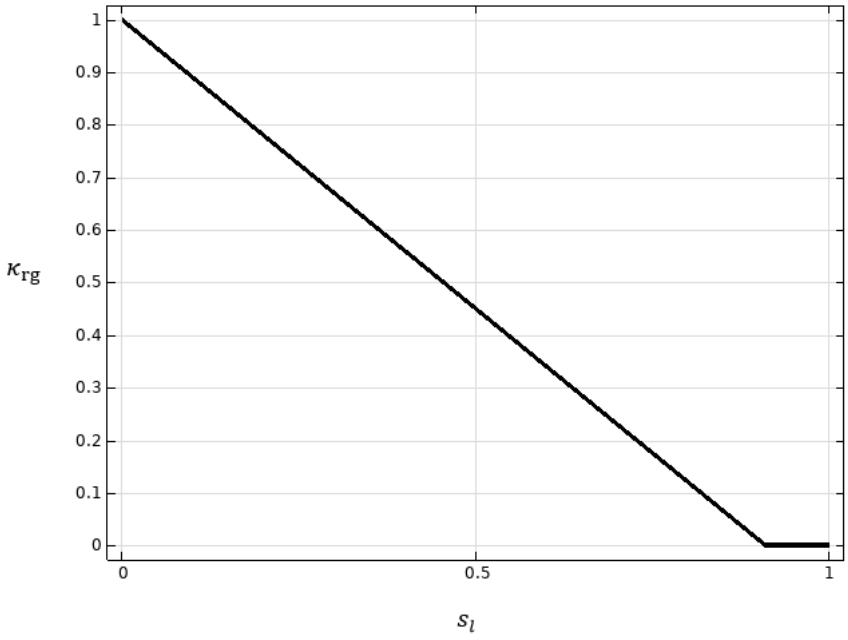

(a)

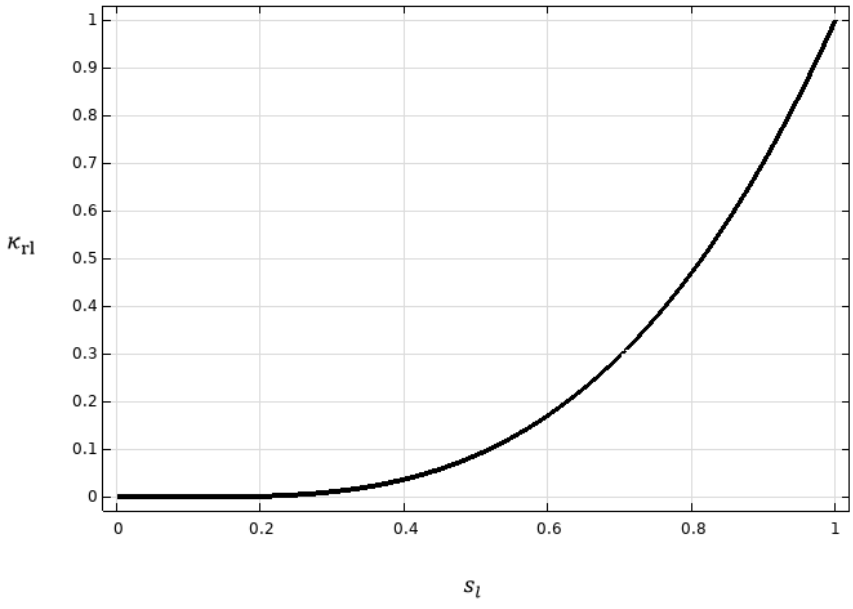

(b)

Fig. 2. Relative permeability: a) gas, b) liquid

Specific heats of various fibres are different but in order of J/kgK. It starts from Glass which is 800 J/kgK to Nylon (PAD 66) which is 1430 J/kgK. The other usual fibres are between this range (Rayon or Viscose, 1260 J/kgK, Wool 1360 J/kgK, Silk 1380 J/kgK, Polyester Terylene 1340 J/kgK, and Asbestos 1050 J/kgK). As well the Thermal conductivity of various fibres are different but in order of 0.1 W/mK. It starts from Silk bats which is 50 to Polytetrafluoroethylene which is 350. The other usual fibres are between this range (PVC 160, Cellulose acetate 230, Nylon 250, Polyester 140, Polyethylene 340, Polypropylene 120, PET 140, Glycerol 290, Cotton cellulose 70, Cotton bats 60, Wool bats 54). Prediction of effective thermal conductivities in many multiphase systems studied by various method such as local volume averaging (system swank from the micro to the macro scale), homogenization of a unit cell in a periodic structure (based on the thermal conductivities base material and void volume fraction) and thermal resistance networks (based on the similarity between electrical conduction and thermal conduction). As there any many length scales in such systems (diameter, length, distance between…) which make difficult a mathematical and analytical solution for the effective thermal conductivity. Table 5 presents porous matrix properties.

Table 5
Porous Matrix Properties.

Parameter	Value	Unit	Description
ε	0.8	-	Porosity
κ	1e-14	m²	Permeability
ks	0.21	W/(m·K)	Porous matrix thermal conductivity
Cp,s	1650	J/(kg·K)	Porous matrix heat capacity
ρs	1528	kg/m³	Porous matrix density

2.6 Thermal Radiation in Participating Media

In outdoor condition, sometimes the textile heated or cooled down by thermal radiation. Numerical calculations of thermal radiative heat transfer aids to optimize the design of a textile. The original thermal radiative heat transfer governing equation is an integro-differential complex equation. Therefore, here some simplified approach is used to solve the thermal radiative heat transfer governing equation coupled with the heat conservation of the system. Between the methods calculating the thermal radiative heat transfer in a gray porous medium shown in Figure 1. Convective cooling by 20°C happens at the top surface of porous media while the radiation is absorbed and transferred inside porous media. Because of thin layer of absorber and computational costs, the P1 method for Radiative Heat Transfer is not used. Although P1 method uses one integration over all wave numbers but there are simpler ways to overcome the problem. The Rosseland approximation (which is for large optical thickness) is used here which is reasonable for medium temperatures as in this model. Implementation of the Rosseland approximation is simple and just needed a nonlinear term in the thermal conductivity at heat conservation of the system. The linearized radiative heat transfer coefficient is added to the thermal conductivity of the porous media as

$$k_{eff} = k + \frac{16\sigma_{SB}}{3a_R}T^3 \tag{11}$$

The mathematical and physical advantage of the above equation (sometimes called the diffusion method) is it can apply through Fourier's second law of conduction.

$$\frac{DT}{Dt} = \frac{\partial T}{\partial t} + u\frac{\partial T}{\partial x} + v\frac{\partial T}{\partial y} = \alpha\left(1 + \frac{16\sigma_{SB}T_{\infty}^{3}}{3ka_{R}}\right)\left(\frac{\partial^{2}T}{\partial x^{2}} + \frac{\partial^{2}T}{\partial y^{2}}\right) \quad (12)$$

The nonlinear coefficient, considered as well, the extinction coefficient (cross section of absorbed or scattered), and the refractive index. The emissivity of skin surface is 0.95. Without the textile the skin will reach higher temperature as the effective heat transfer coefficient for radiation is 4.7 W/m2 in average. Manikin segment radiative coefficients radiative coefficients are foot 4.2-3.9, lower leg 5.4-5.3, thigh 4.6-4.3, pelvis 4.8-4.2, head 3.9-4.1, hand 3.9-4.1, forearm 5.2-4.9, upper arm 4.8-5.2, chest 3.4-4.5, and back 4.6-4.4 for seated and standing conditions respectively.

3. Results

The mathematical model of the simulations in terms of governing equations of mass, momentum, and energy balance for the air and water phases through the porous media are presented. The boundary conditions for temperature are described as well. The grid generation in this study is based on triangulation method. The check for grid independence is presented in table 6. Solutions presented in the previous section are in the Laplace domain. The time domain solutions can be found using numerical inversion methods which has been used extensively in the literature. In the following subsections, the time domain solutions are evaluated. Then, the effects of the various parameters on advective–diffusive mass transfer in porous media are investigated.

3.1 Mesh Independence

Using a proper mesh size is important to resolve the steep gradients at the interface boundaries. Therefore, a customized mesh with boundary layers is used. To get good convergence of the time dependent behavior, first solve the stationary flow equations only. Iteration or convergence errors occur due to the difference between a fully converged solution of a finite number of grid points and a solution that has not fully achieved convergence. As the effect of temperature and mass transfer on fluid flow is neglected one can use stationary solution of fluid flow and applied for transient equation of mass and heat balance. This solution will then be used for the time dependent study step. This approximation neglects the evaporation mass source in the fluid flow computation. No previous benchmark in field exists on verification of the method. Thickness of the fabric- 3D structure of the fabric and surface treatments of the fabric is not considered here.

Mesh configuration related to Table 6 is plotted in Figure 3 for case 4. the relative error defined/computed by L2 norm of temperature in steady state. The influence of the step size (of the time is 5 seconds) on the transient result is negligible for time step less than 10 seconds. the boundary layer element types are used for the top of the channel and porous media than for the entire mesh. a screenshot of the mesh is plotted in figure 3.

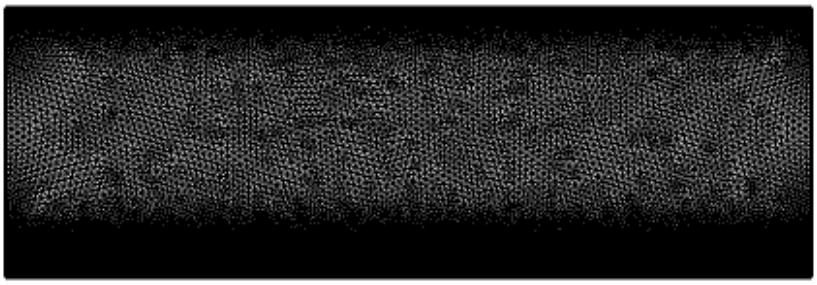

Fig. 3. Grid independence related to Table 6 (Mesh 4)

Table 6
Grid independence for the meshes

	Number of cells	Relative Error of maximum temperature rise in system
Mesh 1	3224	2.78
Mesh 2	4623	2.07
Mesh 3	5654	1.87
Mesh 4	6089	1.17
Mesh 5	6445	0.66
Mesh 6	7087	0

3.2 Temperature

The temperature (Figure 4) shows significant cooling in the whole domain. As the optical path is large the radiation effects in porous media banquet at top surrounding surface of porous media and does not foldaway far through it. A fabric is not only a mesh. The 34.45°C is used here as an interested temperature of body. For various segment skin temperature in neutral stable condition the other values could be obtained. For example, forehead 35.8, cheek 35.2, front neck 35.8, back neck 35.4, chest 35.1 34.5, back 35.3, abdomen 35.3, upper arm 34.2, lower arm 34.6, hand 34.4, left finger 35.3, thigh 34.3, shin 32.9, calf 32.7, foot 33.3. As well in cold stable condition the average of 26.8°C is recommended. For various segment skin temperature in cold stable condition the other values could be obtained. For example, forehead 30.7, cheek 27.7, front neck 33.5, back neck 34.5, chest 30.9, back 32.4, abdomen 28.7, upper arm 24.7, lower arm 27.3, hand 23.1, left finger 21.1, thigh 27.0, shin 26.5, calf 24.3, and foot 21.4. In following Figures 4, there are large areas. If the x-axis and y-axis have meaning of horizontal (skin direction) and vertical directions. Such figure gives no suggestions for design of textiles are given yet.

Estimates based on data-assimilating porous models have several difficulties. First, the model output often does not obey total mass conservation making budget calculations difficult. Second, there is a lack of temperature profile data over the porous caused by the surface flux fields, indicating differences between the models and observations.

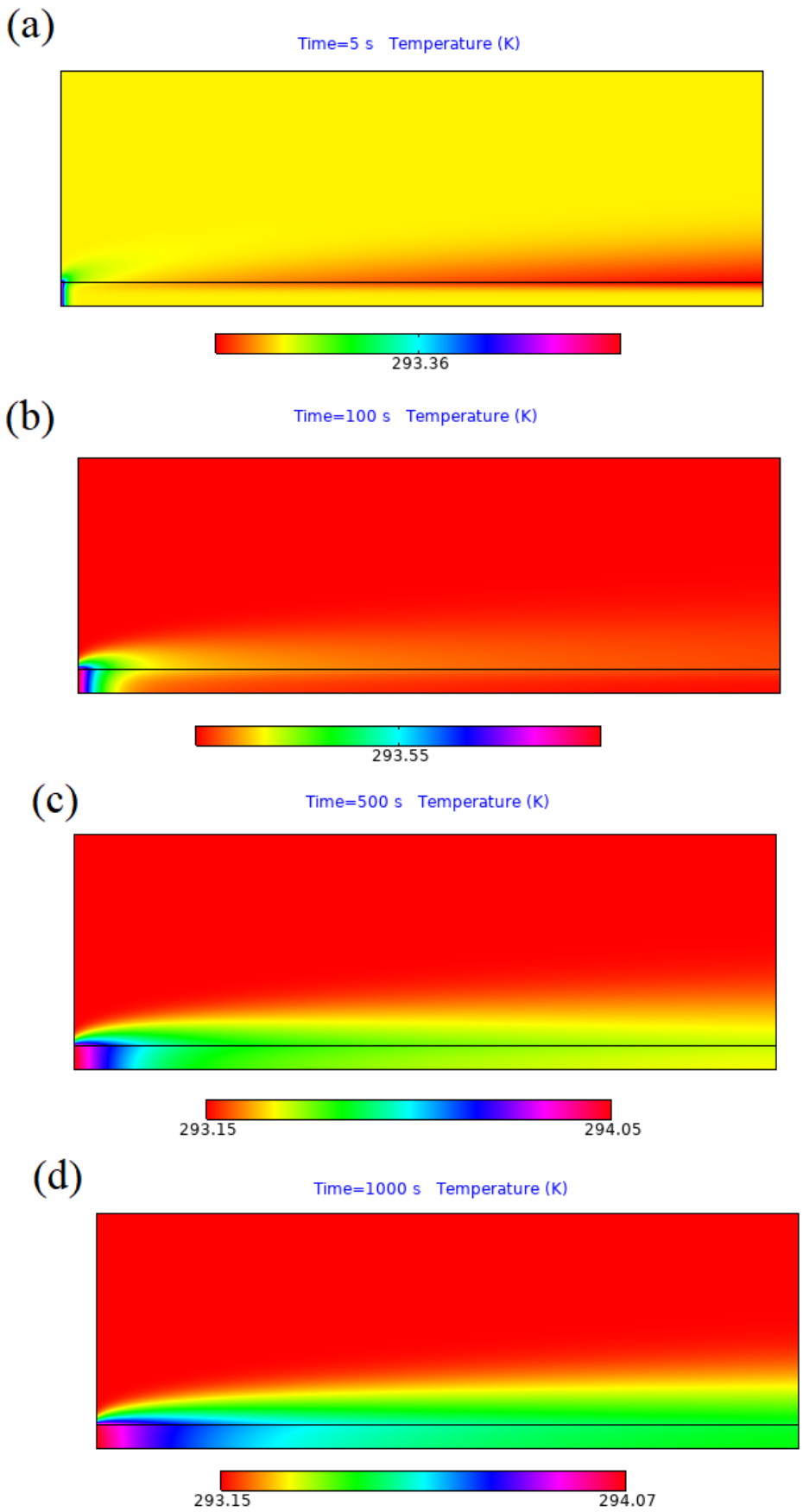
(a)
Time=5 s Temperature (K)
293.36
(b)
Time=100 s Temperature (K)
293.55
(c)
Time=500 s Temperature (K)
293.15
294.05
(d)
Time=1000 s Temperature (K)
293.15
294.07

(e)

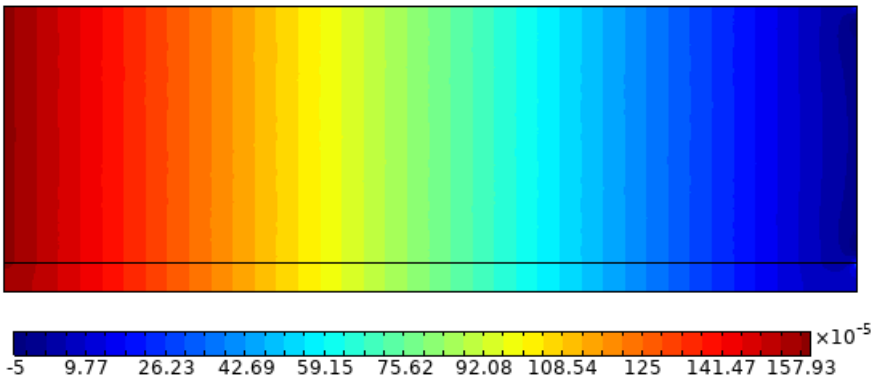

Fig. 4. Temperature field through 1000 seconds: a) t= 5, b) t = 100, c) 500, d) t = 1000 and e) Stationary pressure distribution in Pa

3.3 Pressure

The default pressure contour plot is shown on Figure 3-e. The uniform gradient of pressure profile guarantees the smooth boundary layer flow over the porous medium. Although the various equations described in the paper are predictions about the movement of water, the following pressure distribution shows the linear decrease of pressure through skin direction which make it suitable for the predictions of boundary layer in the actual situation.

3.3.1 Vapor concentration and Influence of Relative Humidity on Drying Behaviour

To measure the optimal design of real textiles under thermos-physiological aspects here the Vapor concentration and influence of relative humidity on drying behavior is studied. Inside the porous domain the relative humidity is close to 100% everywhere (Figure 5). Concentration (mol/m3) through 1000 seconds shows that initial condition at t= 0 changes to the steady state condition soon and concentration profile developed fast. As well, Inside the porous domain the relative humidity is close to 100% everywhere (Figure 6). Relative humidity through 1000 seconds shows that initial condition at t= 0 changes to the steady state condition soon and concentration profile developed fast.

With the intention of studying the influence of environmental water content in air or relative humidity (RH %) on drying performance of textile, some levels of RH are selected. Instead of dry air based on standard RH of 50% and two near values (lower and higher as compared to standard value). Influence of RH on drying time for a constant porous and geometry parameter are performed and plotted in Figure 5. The Figure 7 show that three different RH levels have unimportant variance in their drying actions of the cloths. Figure 8 presents vapour concentration and streamline of concentration flux for various inlet conditions after 1000 seconds: a) RH= 0, b) RH = 0.1, c) RH= 0.5, d) t = RH= 1. As shown although the concentration contours change fast to the steady state, but the mass fluxes are reacted slower. Fabrics in stretched and unstretched condition- e.g., warp/weft could be compared to real situation (e.g., sportswear) which is not considered here.

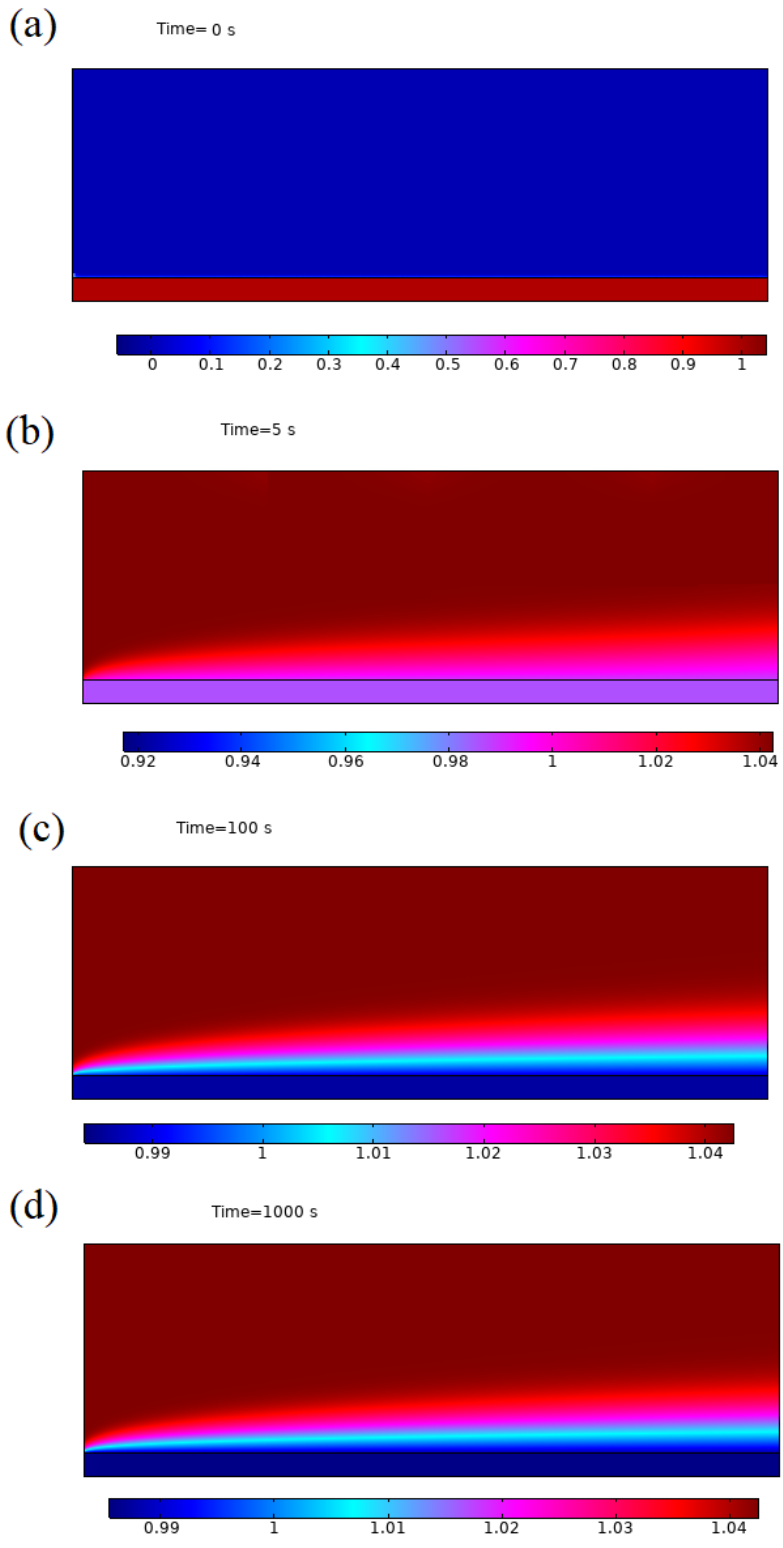

Fig. 5. Concentration (mol/m3) through 1000 seconds: a) t= 0, b) t = 5, c) 100, d) t = 1000

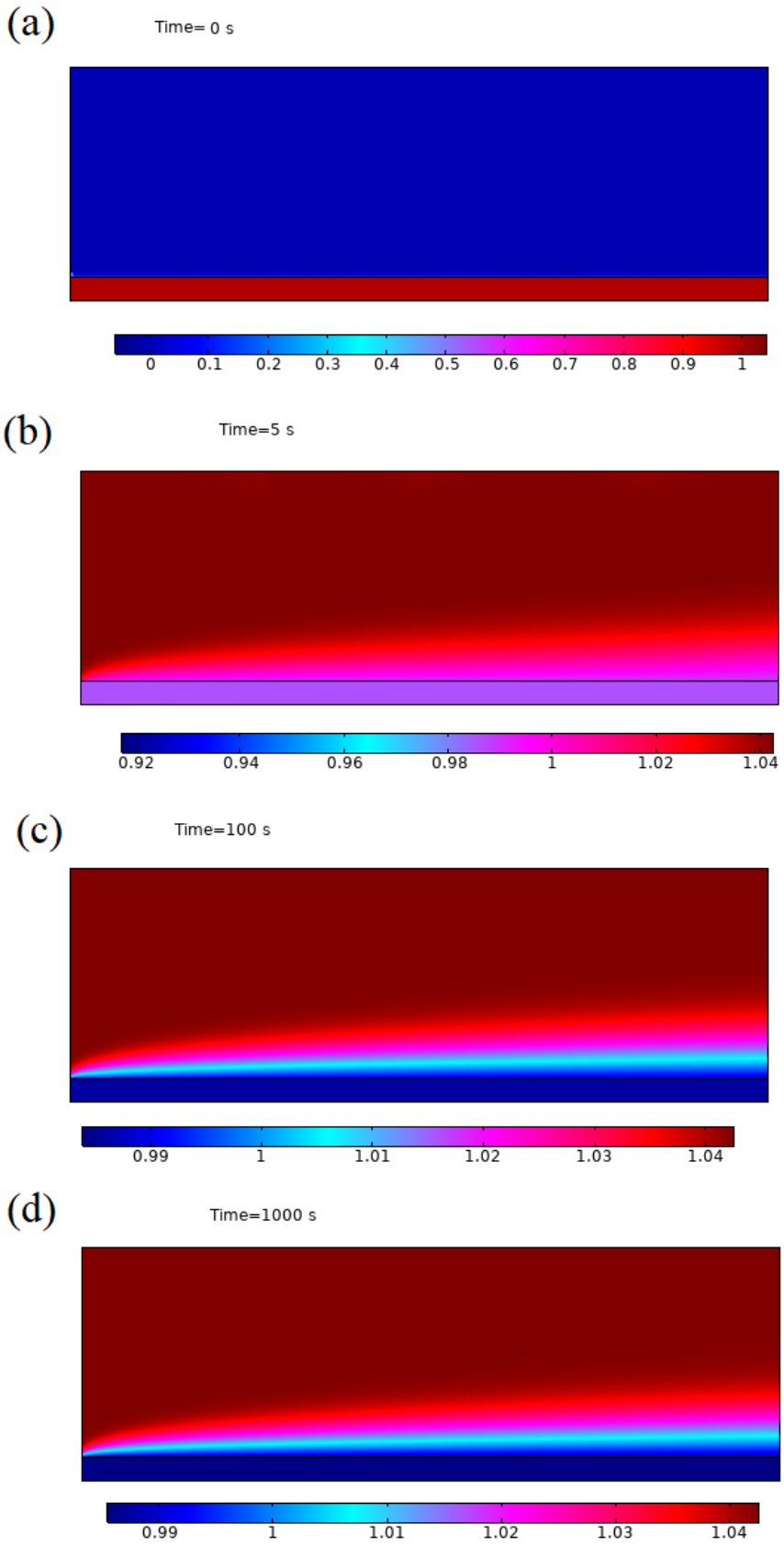

Fig. 6. Relative humidity through 1000 seconds: a) t= 0, b) t = 5, c) 100, d) t = 1000

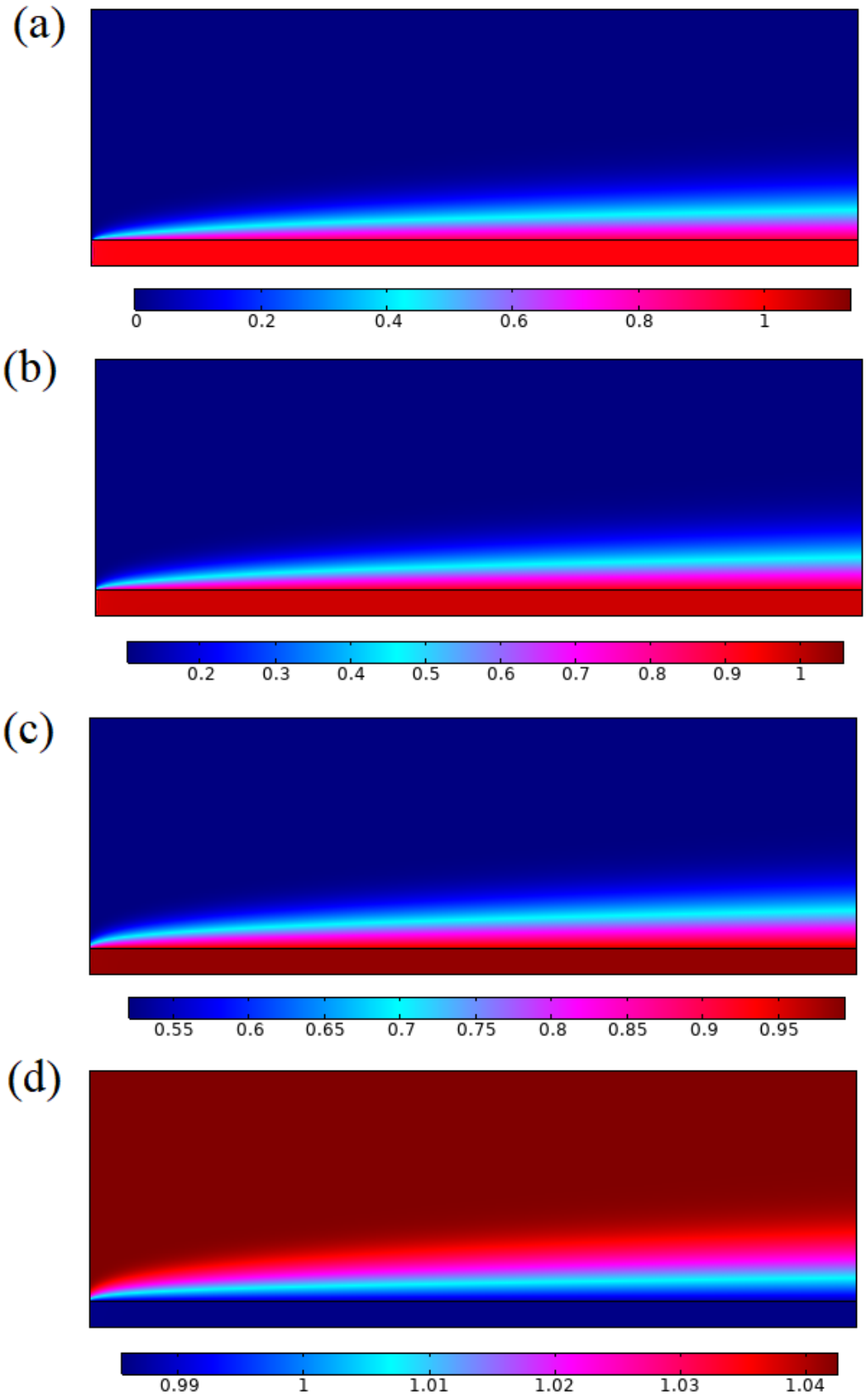

Fig. 7. Relative humidity for various inlet conditions after 1000 seconds: a) RH= 0, b) RH = 0.1, c) RH= 0.5, d) t = RH= 1

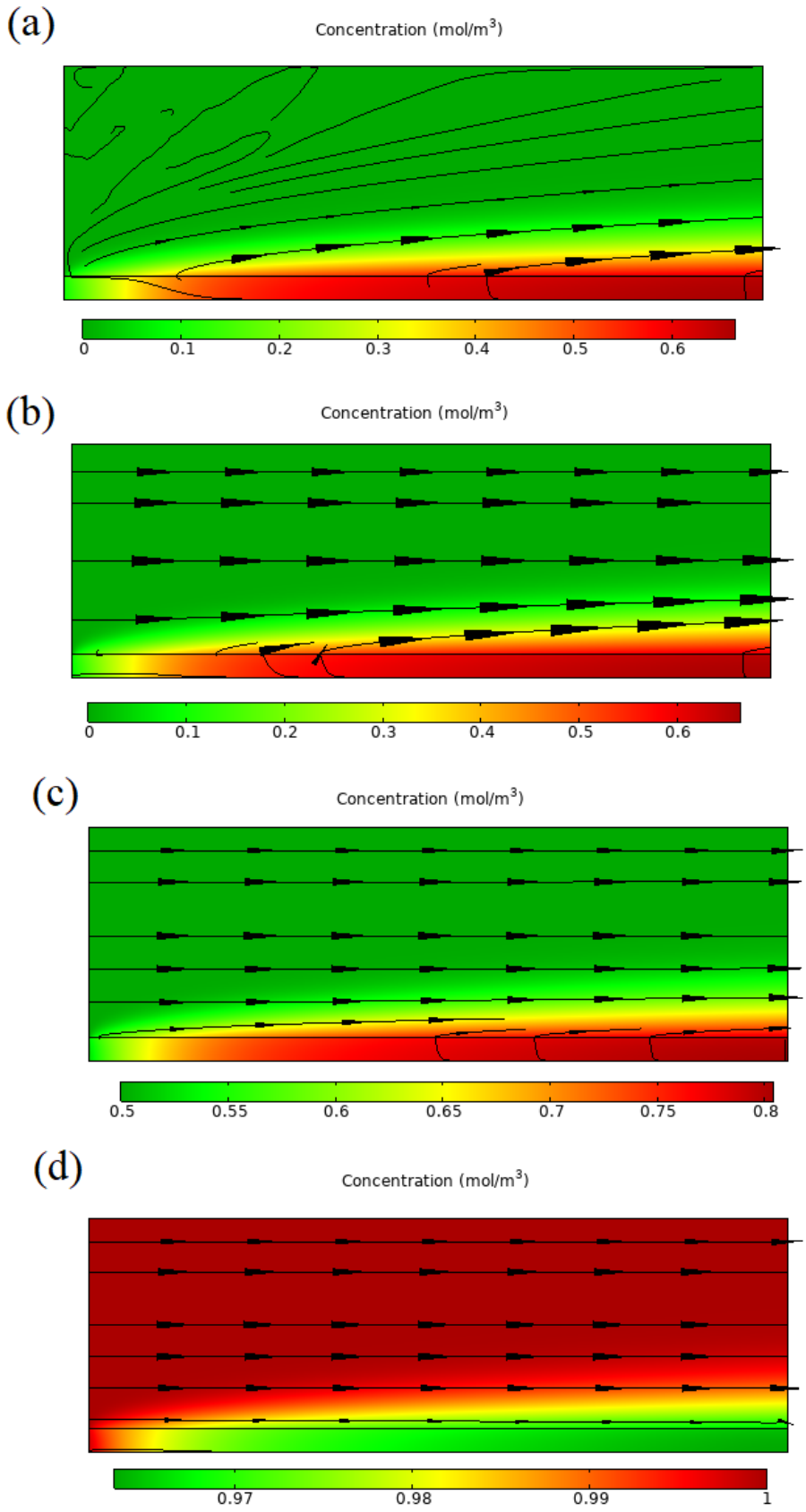

Fig. 8. Vapor concentration and streamline of concentration flux for various inlet conditions after 1000 seconds: a) RH= 0, b) RH = 0.1, c) RH= 0.5, d) t = RH= 1

3.4 Comfort Temperature As A Function Of Porosity Of Medium

With the intention of studying the influence of porosity of the system over surface temperature in steady state interval of 0.1-0.9 of porosity are selected for parameter study. In this research the average surface temperature of 15°C is selected for the human comfort which is correspond to porosity of 0.375. It is good to mentioned that current complex numerical study performed, can be applied to textiles by considering the following figure 9. As shown by increase of surface temperature decrease. Cloth design is (textile structure/design) tight fitted the problem. Sun light radiation could be tested via Hönle device sunlight. A clear structure concerning the investigation program is obtained from figure 9. As well it will give the idea for test set up, conditions with statistical approach in porous media.

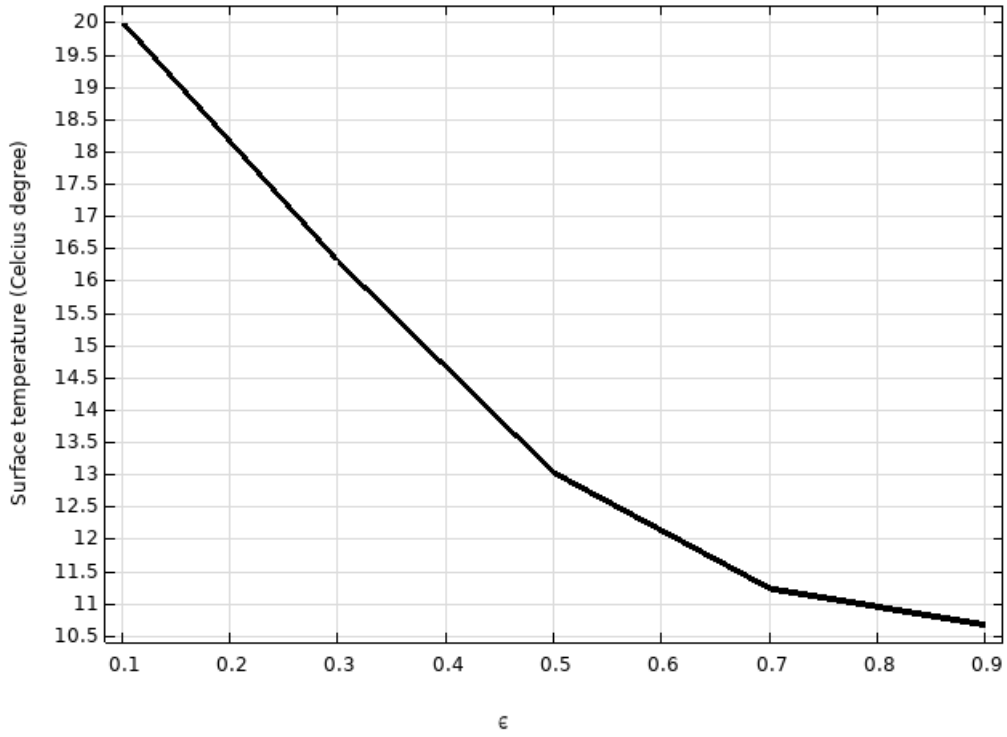

Fig. 9. Surface temperature as a function of porosity

4. Conclusions

This is a study, dedicated to a very complex phenomenon. Though the manuscript presents, in fact, a simulation study on the complex interaction between a textile layer, sweating skin, environmental air and sun radiation.

The common cloth design methods rarely give us instinctual acumens around the effect of all related limits in the textile media. Cloth design is important for human comfort and thermal physiology. The mass and heat transfer from the skin covering play an important role in human thermoregulation and engineering design of textile and dressing. Heat and moisture transfer due to sweating in a clothing system under sun radiation is performed in this study. Governing equations of mass, momentum, and energy balance for the air and water phases through the porous media are solved by finite element method.

Results of temperature, pressure, water vapor concentration, and relative humidity for various time steps are analyzed. As well influence of relative humidity on drying behavior is studied. Finally based on the comfort temperature for skin surface the optimal porosity of medium is obtained.

For further studies it is good to explore the effects of material, fibers, yarn linear density, mesostructured, microstructure of the tissue, etc. This study presents design suggestions and garment improvements. The current method can be used as an algorithm for cloth design for various environmental (velocity, temperature, relative humidity) and material properties (diffusion, porosity, water activity) for desired human comfort. The investigation program could be studied with different fabrics.

Acknowledgement
The author wants to acknowledge the Humboldt institute for Research Fellowship Program of Experienced Researchers and Prof. Dr.-Ing. Ulrich Nieken and M.Sc Lukas Maier for inspiration

References

[1] Datta, A. K. "Porous media approaches to studying simultaneous heat and mass transfer in food processes. I: Problem formulations." *Journal of food engineering* 80, no. 1 (2007): 80-95. https://doi.org/10.1016/j.jfoodeng.2006.05.013
[2] Datta, A. K. "Porous media approaches to studying simultaneous heat and mass transfer in food processes. II: Property data and representative results." *Journal of food engineering* 80, no. 1 (2007): 96-110. https://doi.org/10.1016/j.jfoodeng.2006.05.012
[3] Halder, Amit, Ashish Dhall, and Ashim K. Datta. "Modeling transport in porous media with phase change: applications to food processing." (2011): 031010. https://doi.org/10.1115/1.4002463
[4] Raja, D., M. Senthilkumar, and K. Mani. "Novel device for evaluating sweat evaporation characteristics of woven and knitted fabrics." (2017).
[5] Agarwal, Bhagwan D., Lawrence J. Broutman, and C. W. Bert. "Analysis and performance of fiber composites." (1981): 213-213. https://doi.org/10.1115/1.3157582
[6] Ali, Y. M., and L. C. Zhang. "Relativistic heat conduction." *International journal of heat and mass transfer* 48, no. 12 (2005): 2397-2406. https://doi.org/10.1016/j.ijheatmasstransfer.2005.02.003
[7] Arfken, George B., and Hans J. Weber. "Mathematical methods for physicists." (1999): 165-169. https://doi.org/10.1119/1.19217
[8] Bachmat, Yehuda, and Jacob Bear. "Macroscopic modelling of transport phenomena in porous media. 1: The continuum approach." *Transport in porous media* 1, no. 3 (1986): 213-240. https://doi.org/10.1007/BF00238181
[9] Bear, Jacob, and Yehuda Bachmat. *Introduction to modeling of transport phenomena in porous media*. Vol. 4. Springer Science & Business Media, 2012.
[10] Bear, Jacob, and Jean-Marie Buchlin, eds. *Modelling and applications of transport phenomena in porous media*. Vol. 5. Boston, MA: Kluwer Academic Publishers, 1991. https://doi.org/10.1007/978-94-011-2632-8
[11] Bejan, Adrian, Ibrahim Dincer, Sylvie Lorente, Antonio Miguel, and Heitor Reis. *Porous and complex flow structures in modern technologies*. Springer Science & Business Media, 2004. https://doi.org/10.1007/978-1-4757-4221-3
[12] Bensoussan, Alain, Jacques-Louis Lions, and George Papanicolaou. *Asymptotic analysis for periodic structures*. Vol. 374. American Mathematical Soc., 2011. https://doi.org/10.1090/chel/374
[13] Bird, R. Byron. "Transport phenomena." *Appl. Mech. Rev.* 55, no. 1 (2002): R1-R4. Carbonell, Ruben G., and Stephen Whitaker. "Heat and mass transfer in porous media." In *Fundamentals of transport phenomena in porous media*, pp. 121-198. Springer, Dordrecht, 1984. https://doi.org/10.1007/978-94-009-6175-3_3
[14] CHANG, HSUEH-CHIA. "Multi-scale analysis of effective transport in periodic heterogeneous media." *Chemical Engineering Communications* 15, no. 1-4 (1982): 83-91. https://doi.org/10.1080/00986448208911060
[15] Cheng, Ping, and Chin-Tsau Hsu. "The effective stagnant thermal conductivity of porous media with periodic structures." *Journal of Porous Media* 2, no. 1 (1999). https://doi.org/10.1615/JPorMedia.v2.i1.20
[16] Dasgupta, A., R. K. Agarwal, and S. M. Bhandarkar. "Three-dimensional modeling of woven-fabric composites for effective thermo-mechanical and thermal properties." *Composites science and technology* 56, no. 3 (1996): 209-223. https://doi.org/10.1016/0266-3538(95)00111-5
[17] Whitaker, Stephen. *The method of volume averaging*. Vol. 13. Springer Science & Business Media, 1998. https://doi.org/10.1007/978-94-017-3389-2

[18] Woo, Sang S., Itzhak Shalev, and Roger L. Barker. "Heat and moisture transfer through nonwoven fabrics: Part I: Heat transfer." *Textile Research Journal* 64, no. 3 (1994): 149-162. https://doi.org/10.1177/004051759406400305

[19] Woo, Sang S., Itzhak Shalev, and Roger L. Barker. "Heat and moisture transfer through nonwoven fabrics: Part II: Moisture diffusivity." *Textile Research Journal* 64, no. 4 (1994): 190-197. https://doi.org/10.1177/004051759406400402

[20] Lan, Xiaohua, Yi Wang, Jiebin Peng, Yang Si, Jie Ren, Bin Ding, and Baowen Li. "Designing heat transfer pathways for advanced thermoregulatory textiles." *Materials Today Physics* 17 (2021): 100342. https://doi.org/10.1016/j.mtphys.2021.100342

[21] Ewis, Karem Mahmoud. "Effects of Variable Thermal Conductivity and Grashof Number on Non-Darcian Natural Convection Flow of Viscoelastic Fluids with Non Linear Radiation and Dissipations." *Journal of Advanced Research in Applied Sciences and Engineering Technology* 22, no. 1 (2021): 69-80. https://doi.org/10.37934/araset.22.1.6980

[22] Elsayed, Ahmed M. "Design Optimization of Diffuser Augmented Wind Turbine." *CFD Letters* 13, no. 8 (2021): 45-59. https://doi.org/10.37934/cfdl.13.8.4559

[23] Ahmad, I., M. Faisal, and T. Javed. "Significance of convective Nield's conditions on radiative Casson nanomaterial flow over a bidirectional stretching surface with Arrhenius energy." *Int J Ambient Energy* (2022): 1-12. https://doi.org/10.1080/01430750.2022.2073263

[24] Ahmad, Iftikhar, Muhammad Faisal, K. Loganathan, Muhammad Zaheer Kiyani, and Ngawang Namgyel. "Nonlinear Mixed Convective Bidirectional Dynamics of Double Stratified Radiative Oldroyd-B Nanofluid Flow with Heat Source/Sink and Higher-Order Chemical Reaction." *Mathematical Problems in Engineering* 2022 (2022). https://doi.org/10.1155/2022/9732083

[25] Ahmad, Iftikhar, Muhammad Faisal, Qazi Zan-Ul-Abadin, Tariq Javed, and K. Loganathan. "Unsteady 3D heat transport in hybrid nanofluid containing brick shaped ceria and zinc-oxide nanocomposites with heat source/sink." *Nanocomposites* 8, no. 1 (2022): 1-12. https://doi.org/10.1080/20550324.2021.2008208

[26] Ahmad, Iftikhar, Muhammad Faisal, Qazi Zan-Ul-Abadin, K. Loganathan, Tariq Javed, and Balachandra Pattanaik. "Dynamics of Nanoplatelets in Mixed Convective Radiative Flow of Hybridized Nanofluid Mobilized by Variable Thermal Conditions." *Mathematical Problems in Engineering* 2022 (2022). https://doi.org/10.1155/2022/4417418

[27] Ahmad, Iftikhar, Qazi Zan-Ul-Abadin, Muhammad Faisal, K. Loganathan, Tariq Javed, and Dinesh Kumar Chaudhary. "Prescribed Thermal Activity in the Radiative Bidirectional Flow of Magnetized Hybrid Nanofluid: Keller-Box Approach." *Journal of Nanomaterials* 2022 (2022). https://doi.org/10.1155/2022/5531041

[28] Ahmad, Iftikhar, Qazi Zan-Ul-Abadin, Muhammad Faisal, K. Loganathan, Tariq Javed, and Sonam Gyeltshen. "Entropy analysis in bidirectional hybrid nanofluid containing nanospheres with variable thermal activity." *Journal of Nanomaterials* 2022 (2022). https://doi.org/10.1155/2022/1915185

[29] Ahmad, Iftikhar, Qazi Zan-Ul-Abadin, Muhammad Faisal, K. Loganathan, Tariq Javed, and Ngawang Namgyel. "Convective heat transport in bidirectional water driven hybrid nanofluid using blade shaped Cadmium Telluride and graphite nanoparticles under electromagnetohydrodynamics process." *Journal of Mathematics* 2022 (2022). https://doi.org/10.1155/2022/4471450

[30] Eswaramoorthi, S., S. Divya, Muhammad Faisal, and Ngawang Namgyel. "Entropy and heat transfer analysis for MHD flow of-water-based nanofluid on a heated 3D plate with nonlinear radiation." *Mathematical Problems in Engineering* 2022 (2022). https://doi.org/10.1155/2022/7319988

[31] Eswaramoorthi, S., K. Loganathan, Muhammad Faisal, Thongchai Botmart, and Nehad Ali Shah. "Analytical and numerical investigation of Darcy-Forchheimer flow of a nonlinear-radiative non-Newtonian fluid over a Riga plate with entropy optimization." *Ain Shams Engineering Journal* (2022): 101887. https://doi.org/10.1016/j.asej.2022.101887

[32] Faisal, Muhammad, F. Mabood, and I. A. Badruddin. "On numerical analysis of hydromagnetic radiative Jeffery nanofluid flow by variable thickness surface with activation energy and unsteadiness aspects." *Waves in Random and Complex Media* (2022): 1-19. https://doi.org/10.1080/17455030.2022.2075049

[33] Faisal, Muhammad, F. Mabood, Kanayo Kenneth Asogwa, and I. A. Badruddin. "Bidirectional radiative transport of magnetic Maxwell nanofluid mobilized by Arrhenius energy and prescribed thermal/concentration conditions: Significance of Ludwig-Soret and pedesis effects." *Ain Shams Engineering Journal* (2022): 101933. https://doi.org/10.1016/j.asej.2022.101933

[34] Jamalabadi, M. "MD simulation of brownian motion of buckminsterfullerene trapping in nano-optical tweezers." *Int. J. Opt. Appl* 5 (2015): 161-167.

[35] Jamalabadi, MY Abdollahzadeh, and J. Park. "Electro-magnetic ship propulsion stability under gusts." *International Journal of Sciences: Basic and Applied Research Sciences* 14 (2014): 421-427.